Coupled Marchenko equations for electromagnetic Green's function retrieval and imaging

Evert Slob and Kees Wapenaar, Delft University of Technology

SUMMARY

Recently a new theory has been developed to retrieve a wavefield generated by a source on the surface and recorded at a point in the subsurface without the need for a receiver at that subsurface location. The scheme is presented for three-dimensional wavefields. It decomposes the electromagnetic field in up- and downgoing electric fields and in TE- and TM-modes. Each mode can be treated separately to construct the Green's function. We derive two coupled Marchenko equations from which the up- and downgoing Green's functions can be obtained. These two directional Green's functions have applications in true-amplitude subsurface imaging without effects from internal multiple reflections.

INTRODUCTION

Recent developments for seismic data (Broggini *et al.* , 2012) and the mathematical framework of Wapenaar *et al.* (2013b) makes it possible to place a virtual receiver in the subsurface and compute the corresponding Green's function without having a physical source or receiver at that location. Here we present a three-dimensional electromagnetic scheme similar to the acoustic scheme of Wapenaar *et al.* (2013). The electromagnetic scheme can be applied to a layered medium where the layers can be characterized by different horizontal and vertical electric permittivity and magnetic permeability values that vary smoothly in the horizontal direction inside each layer. We decompose the recorded wavefield into up- and downgoing waves separated in TE- and TM-modes, which can be treated independently after the first step. We then define a focusing wavefield that focuses at a particular location in the subsurface. This upgoing and downgoing parts of the focusing wavefield can be found separately from the measured reflection data and an estimate of the direct arrival from the surface source point to the subsurface focusing point. This leads to Green's function retrieval corresponding of a virtual vertical radar profile. The up- and downgoing wave fields at the virtual receiver level are obtained separately and can be used in an imaging scheme that creates a true-amplitude subsurface image free from ghost effects due to internal mutliples. A numerical example illustrates the Green's function retrieval.

WAVE FIELD DECOMPOSITION

We start with Maxwell's equations in space-frequency domain (Kong, 1972)

$$\eta^{(\mathrm{V})}\hat{E}_z = -\hat{J}^e_z + \hat{z}\cdot(\nabla_T\times\hat{\mathbf{H}}_T), \tag{1}$$

$$\zeta^{(\mathrm{V})}\hat{H}_z = -\hat{J}^m_z - \hat{z}\cdot(\nabla_T\times\hat{\mathbf{E}}_T), \tag{2}$$

$$\eta\hat{\mathbf{E}}_T = -\hat{\mathbf{J}}^e_T + \hat{z}\times\partial_z\hat{\mathbf{H}}_T + \nabla_T\times\hat{z}\hat{H}_z, \tag{3}$$

$$\zeta\hat{\mathbf{H}}_T = -\hat{\mathbf{J}}^m_T - \hat{z}\times\partial_z\hat{\mathbf{E}}_T - \nabla_T\times\hat{z}\hat{E}_z, \tag{4}$$

where $\hat{E}_z,\hat{H}_z$ and $\hat{J}^e_z,\hat{J}^m_z$ denote the vertical components of the electric and magnetic fields and sources, $\hat{\mathbf{E}}_T,\hat{\mathbf{H}}_T$ and $\hat{\mathbf{J}}^e_T,\hat{\mathbf{J}}^m_T$ the electric and magnetic field and source vectors with subscript $_T$ meaning that the vectors contain only the horizontal components, e.g. $\hat{\mathbf{E}}_T=(\hat{E}_x,\hat{E}_y,0)$, and ∇_T denotes the vector containing the spatial derivatives to the horizontal coordinates. The electric and magnetic medium parameters in the horizontal and vertical directions are given by $\eta=\sigma+\mathrm{i}\omega\varepsilon,\zeta=\mathrm{i}\omega\mu$, $\eta^{(\mathrm{V})}=\sigma^{(\mathrm{V})}+\mathrm{i}\omega\varepsilon^{(\mathrm{V})},\zeta^{(\mathrm{V})}=\mathrm{i}\omega\mu^{(\mathrm{V})}$, respectively. The vertical derivative is denoted ∂_z and $\hat{z}$ denotes the unit vector in the vertical direction and points downward. In a vertical transverse isotropic (VTI) layered medium the TE- and TM-modes are independent modes that can be separated under the condition that lateral variations are smooth, $|\zeta\hat{z}\cdot(\nabla_T\times\hat{\mathbf{H}}_T)|\gg|\hat{z}\cdot(\hat{\mathbf{H}}_T\times\nabla_T\zeta)|$ and $|\eta\hat{z}\cdot(\nabla_T\times\hat{\mathbf{E}}_T)|\gg|\hat{z}\cdot(\hat{\mathbf{E}}_T\times\nabla_T\eta)|$. We now assume this is the case and show the wave fields can be solved for separately after which the electric and magnetic fields can be found by combining the two solutions. Equation 1 represents the TM-mode while equation 2 represents the TE-mode. These two modes can be separated by considering scalar TE-mode, $\hat{\mathscr{E}}_1,\hat{\mathscr{H}}_1$, and TM-mode, $\hat{\mathscr{E}}_2,\hat{\mathscr{H}}_2$, fields given by

$$\hat{\mathscr{E}}_1 = -\hat{z}\cdot\left(\nabla_T\times\hat{\mathbf{E}}_T\right), \qquad \hat{\mathscr{H}}_1 = \nabla_T\cdot\hat{\mathbf{H}}_T, \tag{5}$$

$$\hat{\mathscr{E}}_2 = \nabla_T\cdot\hat{\mathbf{E}}_T, \qquad \hat{\mathscr{H}}_2 = \hat{z}\cdot\left(\nabla_T\times\hat{\mathbf{H}}_T\right). \tag{6}$$

These fields are obtained by applying the horizontal divergence, $\nabla_T\cdot$, and the vertical components of the horizontal curl, $\hat{z}\cdot(\nabla\times\bullet)$, to equations 3 and 4, where $\bullet$ stands for the field on which the spatial derivative should operate. The sources are then given by

$$\hat{\mathscr{J}}_1 = \begin{pmatrix} -\nabla_T\cdot\hat{\mathbf{J}}^m_T \\ \hat{z}\cdot(\nabla_T\times\hat{\mathbf{J}}^e_T) - \nabla_T\cdot\nabla_T(\zeta^v)^{-1}\hat{J}^m_z, \end{pmatrix}, \tag{7}$$

$$\hat{\mathscr{J}}_2 = \begin{pmatrix} -\nabla_T\cdot\hat{\mathbf{J}}^e_T \\ -\hat{z}\cdot(\nabla_T\times\hat{\mathbf{J}}^m_T) - \nabla_T\cdot\nabla_T(\eta^v)^{-1}\hat{J}^e_z. \end{pmatrix}, \tag{8}$$

Now the can write the TE-and TM-mode field equations as a matrix vector equation given by

$$\partial_z\hat{\mathbf{F}}_{1,2} + \hat{\mathbf{A}}_{1,2}\hat{\mathbf{F}}_{1,2} = \hat{\mathscr{J}}_{1,2}. \tag{9}$$

The TE-mode field equations are obtained when we take $\hat{\mathbf{F}}_1 = (\hat{\mathscr{E}}_1,\hat{\mathscr{H}}_1)^t$, where ^{t} denotes matrix transposition, and the TM-mode equations are obtained with $\hat{\mathbf{F}}_2=(\hat{\mathscr{H}}_2,\hat{\mathscr{E}}_2)^t$, with the source vectors defined in equations 7 and 8. The system matrices are given by

$$\hat{\mathbf{A}}_1 = \begin{pmatrix} 0 & \zeta \\ \zeta^{-1}\Gamma_1^2 & 0 \end{pmatrix}, \quad \hat{\mathbf{A}}_2 = \begin{pmatrix} 0 & \eta \\ \eta^{-1}\Gamma_2^2 & 0 \end{pmatrix}, \tag{10}$$

where the vertical wave numbers are operators given by $\Gamma_1^2 = \gamma^2 - \zeta\nabla_T\cdot\nabla_T((\zeta^{(\mathrm{V})})^{-1}\bullet)$, and $\Gamma_2^2=\gamma^2-\eta\nabla_T\cdot\nabla_T((\eta^{(\mathrm{V})})^{-1}\bullet)$, with $\gamma^2=\eta\zeta$. It is noted that the TE-mode does not depend on $\eta^{(\mathrm{V})}$ while the TM-mode does not depend on $\zeta^{(\mathrm{V})}$. Solving

the TE-mode problem directly solves the TM-mode problem based on electromagnetic equivalence.

From here on only the TE-mode is used and we drop the subscript $_1$ in the remainder of this paper. Results obtained for the TE-mode similarly apply to the TM-mode. The electric field at any depth level consists of an upgoing and a downgoing field

$$\hat{\mathscr{E}}(\mathbf{x},\omega) = \hat{\mathscr{E}}^{+}(\mathbf{x},\omega) + \hat{\mathscr{E}}^{-}(\mathbf{x},\omega), \tag{11}$$

where the superscript $^+$ denotes the downgoing field and $^-$ denotes the upgoing field. At a particular depth level, e.g., z_i, we use $\mathbf{x}_i = (\mathbf{x}_T, z_i)$. At this depth level, the electric field reflection response, $\hat{R}$ is defined in terms of the upgoing and downgoing wavefields as

$$\hat{\mathscr{E}}^{-}(\mathbf{x}_i,\omega) = \int_{\partial\mathbb{D}_i} \hat{R}(\mathbf{x}_i,\mathbf{x}_i',\omega)\hat{\mathscr{E}}^{+}(\mathbf{x}_i',\omega)\mathrm{d}^2\mathbf{x}_T'. \tag{12}$$

Outside the source domain the corresponding magnetic field can be written according to the first row equation from equation 9 as

$$\hat{\mathscr{H}}(\mathbf{x},\omega) = -\zeta^{-1}\left(\partial_z\hat{\mathscr{E}}^{+}(\mathbf{x},\omega) + \partial_z\hat{\mathscr{E}}^{-}(\mathbf{x},\omega)\right). \tag{13}$$

With these equations we have decomposed Maxwell's equations into TE- and TM-modes and into up- and downgoing electric fields. The magnetic field is proportional to the vertical derivative of the electric field.

GREEN'S FUNCTION RETRIEVAL FROM REFLECTION DATA

At the receiver level we record the horizontal electric and magnetic field components. This can be in the air or on the surface and the recorded fields can be decomposed according to the scheme in the previous section from which we select the TE-mode upgoing and downgoing field for data driven wavefield extrapolation in the subsurface. For these field quantities the reciprocity theorems of the time-convolution and time-correlation types can be used to obtain relations between the fields in two different states, labeled A and B. We apply reciprocity to a domain that has two horizontal boundaries of infinite extent at depth levels z_r and z_i, both located below the source depth level and $z_i > z_r$. Between the two depth levels we take the medium in both states the same and no sources exist inside the domain or on the boundaries. In that case the reciprocity relations are given by (de Hoop, 1995)

$$\begin{aligned}\int_{\partial\mathbb{D}_r} [\hat{\mathscr{E}}_A(\mathbf{x}_r,\omega)\hat{\mathscr{H}}_B(\mathbf{x}_r,\omega) - \hat{\mathscr{H}}_A(\mathbf{x}_r,\omega)\hat{\mathscr{E}}_B(\mathbf{x}_r,\omega)]\mathrm{d}\mathbf{x}_T = \\ \int_{\partial\mathbb{D}_i} [\hat{\mathscr{E}}_A(\mathbf{x}_i,\omega)\hat{\mathscr{H}}_B(\mathbf{x}_i,\omega) - \hat{\mathscr{H}}_A(\mathbf{x}_i,\omega)\hat{\mathscr{E}}_B(\mathbf{x}_i,\omega)]\mathrm{d}\mathbf{x}_T,\end{aligned} \tag{14}$$

and

$$\begin{aligned}&\int_{\partial\mathbb{D}_r} [\hat{\mathscr{E}}_A^{*}(\mathbf{x}_r,\omega)\hat{\mathscr{H}}_B(\mathbf{x}_r,\omega) + \hat{\mathscr{H}}_A^{*}(\mathbf{x}_r,\omega)\hat{\mathscr{E}}_B(\mathbf{x}_r,\omega)]\mathrm{d}\mathbf{x}_T \\ &= \int_{\partial\mathbb{D}_i} [\hat{\mathscr{E}}_A^{*}(\mathbf{x}_i,\omega)\hat{\mathscr{H}}_B(\mathbf{x}_i,\omega) + \hat{\mathscr{H}}_A^{*}(\mathbf{x}_i,\omega)\hat{\mathscr{E}}_B(\mathbf{x}_i,\omega)]\mathrm{d}\mathbf{x}_T \\ &\quad + 2\int_{\mathbb{D}} \Re\{\sigma(\mathbf{x})\}\hat{\mathscr{E}}_A^{*}(\mathbf{x},\omega)\cdot\hat{\mathscr{E}}_B(\mathbf{x},\omega)\mathrm{d}^3\mathbf{x}.\end{aligned} \tag{15}$$

Both equations 14 and 15 are exact and the second integral in the right-hand side of equation 15 vanishes when the electric losses can be neglected. In the remainder we assume losses can be ignored. We write all functions in terms of upgoing and downgoing electric fields according to equations 11 and 13 and substitute them in equations 14 and 15 leading to

$$\begin{aligned}&-\int_{\partial\mathbb{D}_r} \zeta^{-1}[\hat{\mathscr{E}}_A^{+}(\mathbf{x}_r)\partial_z\hat{\mathscr{E}}_B^{-}(\mathbf{x}_r) + \hat{\mathscr{E}}_A^{-}(\mathbf{x}_r)\partial_z\hat{\mathscr{E}}_B^{+}(\mathbf{x}_r)]\mathrm{d}\mathbf{x}_T \\ &= \int_{\partial\mathbb{D}_i} \zeta^{-1}[\hat{\mathscr{E}}_B^{+}(\mathbf{x}_i)\partial_z\hat{\mathscr{E}}_A^{-}(\mathbf{x}_i) + \hat{\mathscr{E}}_B^{-}(\mathbf{x}_i)\partial_z\hat{\mathscr{E}}_A^{+}(\mathbf{x}_i)]\mathrm{d}\mathbf{x}_T,\end{aligned} \tag{16}$$

and

$$\begin{aligned}&-\int_{\partial\mathbb{D}_r} \zeta^{-1}[[\hat{\mathscr{E}}_A^{+}(\mathbf{x}_r)]^{*}\partial_z\hat{\mathscr{E}}_B^{+}(\mathbf{x}_r) + [\hat{\mathscr{E}}_A^{-}(\mathbf{x}_r)]^{*}\partial_z\hat{\mathscr{E}}_B^{-}(\mathbf{x}_r)]\mathrm{d}\mathbf{x}_T \\ &= \int_{\partial\mathbb{D}_i} \zeta^{-1}[\hat{\mathscr{E}}_B^{+}(\mathbf{x}_i)\partial_z[\hat{\mathscr{E}}_A^{+}(\mathbf{x}_i)]^{*} + [\hat{\mathscr{E}}_B^{-}(\mathbf{x}_i)]^{*}\partial_z[\hat{\mathscr{E}}_A^{-}(\mathbf{x}_i)]^{*}]\mathrm{d}\mathbf{x}_T,\end{aligned} \tag{17}$$

where the explicit dependence on frequency has been omitted for brevity. These equations have been obtained by assuming that the permeability and permittivity at the depth level z_i have zero vertical derivative and are continuously differentiable in horizontal direction, while for equation 17 an additional approximation is made by ignoring evanescent waves at depth level z_i, as described in Appendix B in Wapenaar & Berkhout (1989). This has the consequence that all results should be understood in the spatially band limited sense.

In state A we take the medium between z_r and z_i the same as the actual medium, while above the receiver level and below z_i it is homogeneous with the medium parameters of the actual medium at those depth levels. In this reduced medium we define a focusing electric wavefield, $\hat{e}(\mathbf{x},\mathbf{x}_i',\omega)$, that focuses at a point $\mathbf{x}_i'$ at depth level z_i. Hence at the receiver level we have

$$\hat{\mathscr{E}}_A(\mathbf{x}_r,\omega) = \hat{e}^{+}(\mathbf{x}_r,\mathbf{x}_i',\omega) + \hat{e}^{-}(\mathbf{x}_r,\mathbf{x}_i',\omega), \tag{18}$$

and the focusing condition is given by

$$\partial_z\hat{\mathscr{E}}_A^{+}(\mathbf{x}_i,\mathbf{x}_i',\omega) = -\tfrac{1}{2}\zeta(\mathbf{x}_i')\delta(\mathbf{x}_T - \mathbf{x}_T'), \tag{19}$$

which implies that the wavefield focuses in $\mathbf{x}_i = \mathbf{x}_i'$ after which it propagates downwards as a diverging wavefield and there is no upgoing wavefield below depth level z_i, see Figure 1(a). In state B we take the actual medium and consider the actual measurements with a source at infinitesimal distance above the receivers and receivers at z_r. At the receiver level we assume the horizontal components of the electric and magnetic fields are measured. We then apply the decomposition scheme and in the TE-mode we apply multidimensional deconvolution to find the reflection response from equation 12. After this step we have obtained a wavefield that is characterized by a downgoing source and upgoing reflection response given by

$$\partial_z\hat{\mathscr{E}}_B^{+}(\mathbf{x}_r,\mathbf{x}_r',\omega) = -\tfrac{1}{2}\zeta(\mathbf{x}_r')\delta(\mathbf{x}_{T,r} - \mathbf{x}_{T,r}'), \tag{20}$$

$$\partial_z\hat{\mathscr{E}}_B^{-}(\mathbf{x}_r,\mathbf{x}_r',\omega) = \tfrac{1}{2}\zeta(\mathbf{x}_r)\hat{R}(\mathbf{x}_r',\mathbf{x}_r,\omega). \tag{21}$$

At the depth level z_i we write the electric field in up- and downgoing electric field Green's functions as

$$\hat{\mathscr{E}}_B(\mathbf{x}_i,\omega) = \hat{G}^{+}(\mathbf{x}_i,\mathbf{x}_r',\omega) + \hat{G}^{-}(\mathbf{x}_i,\mathbf{x}_r',\omega), \tag{22}$$

as depicted in Figure 1(b). Substituting these choices for the wavefields in both states in equations 16 and 17 leads to

$$\int_{\partial\mathbb{D}_r} \hat{e}^+(\mathbf{x}_r',\mathbf{x}_i,\omega)R(\mathbf{x}_r,\mathbf{x}_r',\omega)\mathrm{d}\mathbf{x}_T' - \hat{e}^-(\mathbf{x}_r,\mathbf{x}_i,\omega) = \hat{G}^-(\mathbf{x}_i,\mathbf{x}_r,\omega), \quad (23)$$

$$-\int_{\partial\mathbb{D}_r} [\hat{e}^-(\mathbf{x}_r',\mathbf{x}_i,\omega)]^*\hat{R}(\mathbf{x}_r,\mathbf{x}_r',\omega)\mathrm{d}\mathbf{x}_T' + [\hat{e}^+(\mathbf{x}_r,\mathbf{x}_i,\omega)]^* = \hat{G}^+(\mathbf{x}_i,\mathbf{x}_r,\omega), \quad (24)$$

where we dropped the primes on $\mathbf{x}_i$. Equations 23 and 24 represent the upgoing and downgoing electric field at a receiver location $\mathbf{x}_i$, generated by an acoustic source at $\mathbf{x}_r$, in terms of forward and inverse extrapolating wavefields that focus at the receiver point $\mathbf{x}_i$, and the measured electric reflection response. These two equations are coupled by the up- and downgoing focusing wavefield $\hat{e}^{\pm}$.

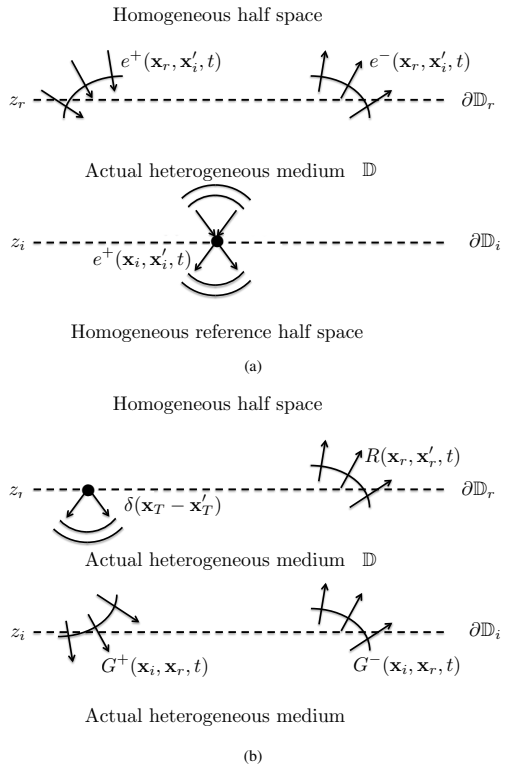

Figure 1: (a) Electric Field normalized focusing wavefield, (b) Electric field normalized Green's functions as necessary in the reciprocity relations.

In the time domain equivalents of equations 23 and 24 the reflection response and electric field Green's functions are causal time functions. The focusing wavefield is a non-causal time function, but exists only in a symmetric time-interval (Slob *et al.* , 2013). The downgoing part of the focusing field focuses at $\mathbf{x}_i'$ at $t=0$ and the arrival time at the receiver level is therefore $t=-t_d(\mathbf{x}_i,\mathbf{x}_r)$ and it is zero after $t \geq t_d(\mathbf{x}_i,\mathbf{x}_r)$. Because e^- is the reflection response generated by e^+ the upgoing part of the focusing wavefield at the receiver level is zero in the interval $|t| \geq t_d(\mathbf{x}_i,\mathbf{x}_r)$. This can be exploited by transforming the equation to the time domain. They are given by

$$G^-(\mathbf{x}_i,\mathbf{x}_r,t) = -e^-(\mathbf{x}_r,\mathbf{x}_i,t) + \int_{\partial\mathbb{D}_r}\int_{t'=-t_d}^{t} e^+(\mathbf{x}_r',\mathbf{x}_i,t')R(\mathbf{x}_r,\mathbf{x}_r',t-t')\mathrm{d}t'\mathrm{d}\mathbf{x}_T', \quad (25)$$

$$G^+(\mathbf{x}_i,\mathbf{x}_r,t) = e^+(\mathbf{x}_r,\mathbf{x}_i,-t) - \int_{\partial\mathbb{D}_r}\int_{t'=-t_d}^{t} e^-(\mathbf{x}_r',\mathbf{x}_i,-t')R(\mathbf{x}_r,\mathbf{x}_r',t-t')\mathrm{d}t'\mathrm{d}\mathbf{x}_T', \quad (26)$$

where the lower time limit in the integrals is $t_d = t_d(\mathbf{x}_i,\mathbf{x}_r')$ and causality of the reflection response determines the upper limit of the time integrals. The Green's functions are zero valued for $t < t_d(\mathbf{x}_i,\mathbf{x}_r)$, while the first arrival is the direct transmission event between $\mathbf{x}_i$ and $\mathbf{x}_r$ hence for all time instances $t < t_d(\mathbf{x}_i,\mathbf{x}_r)$ equations 25 and 26 can be used to solve for the focusing wavefield. The time-instant $t = t_d(\mathbf{x}_i,\mathbf{x}_r)$ cannot be used while the direct arrival of the downgoing part of the focusing wavefield is non-zero at that time-instant. Therefore an estimate of this direct arrival should be obtained. This can be done by building a background velocity model directly from the data. Let us split up the downgoing wavefield in a direct part, $e_d^+(\mathbf{x}_r,\mathbf{x}_i,t)$, and a coda, $e_c^+(\mathbf{x}_r,\mathbf{x}_i,t)$, following the direct part where the coda is zero for $t=-t_d(\mathbf{x}_i,\mathbf{x}_r)$. We then have

$$e^-(\mathbf{x}_r,\mathbf{x}_i,t) = e_0^-(\mathbf{x}_r,\mathbf{x}_i,t) + \int_{\partial\mathbb{D}_r}\int_{t'=-t_d}^{t} e_c^+(\mathbf{x}_r',\mathbf{x}_i,t')R(\mathbf{x}_r,\mathbf{x}_r',t-t')\mathrm{d}t'\mathrm{d}\mathbf{x}_T', \quad (27)$$

$$e_c^+(\mathbf{x}_r,\mathbf{x}_i,-t) = \int_{\partial\mathbb{D}_r}\int_{t'=-t_d}^{t} e^-(\mathbf{x}_r',\mathbf{x}_i,-t')R(\mathbf{x}_r,\mathbf{x}_r',t-t')\mathrm{d}t'\mathrm{d}\mathbf{x}_T', \quad (28)$$

where e_0^- is given by

$$e_0^-(\mathbf{x}_r,\mathbf{x}_i,t) = \int_{\partial\mathbb{D}_r}\int_{t'=-t_d}^{t} e_d^+(\mathbf{x}_r',\mathbf{x}_i,t')R(\mathbf{x}_r,\mathbf{x}_r',t-t')\mathrm{d}t'\mathrm{d}\mathbf{x}_T'. \quad (29)$$

Equations 27 and 28 are the coupled single-sided Marchenko-type equations from which $e_c^+(\mathbf{x}_I,x_r,t)$ and $e^-(\mathbf{x}_i,\mathbf{x}_r,t)$ can be computed. This can be done through an iterative scheme or by solving the resulting matrix vector equation by an inversion procedure. Numerical experience shows that the iterative scheme converges very fast by first assuming that $e_c^+(\mathbf{x}_i,\mathbf{x}_r,t) = 0$. We initialize and compute $e_0^-(\mathbf{x}_i,\mathbf{x}_r,t)$, use it in equation 28 to compute the first order term $e_{c;1}^+(\mathbf{x}_i,\mathbf{x}_r,t)$, which can then be used in equation 27 to compute the first order term $e_1^-(\mathbf{x}_i,\mathbf{x}_r,t)$, and so on. Once the focusing wavefield has been found the Green's functions can be computed from equations 25 and 26. It is interesting to note that unlike other Green's function retrieval methods (Weaver & Lobkis, 2001; Wapenaar, 2004; Slob *et al.* , 2007), both upgoing and downgoing electric fields at a subsurface location $\mathbf{x}_i$ generated by an electric source at the receiver level $\mathbf{x}_r$ can be obtained without having a receiver at the subsurface location $\mathbf{x}_i$. By adding equations 27 and 28 a single Marchenko equation is obtained from which $e^+(\mathbf{x}_r,\mathbf{x}_i,t) - e^-(\mathbf{x}_r,\mathbf{x}_i,-t)$ is obtained and from which the total Green's function can be obtained (Wapenaar *et al.* , 2013a).

Table 1: Values for relative permittivity, ε_r, and thickness, h.

ε_r (-)	1.0	3.9	2.4	9.0	16.1	12.3	9.1
h (m)	0.15	1.75	0.25	1.0	1.3	0.75	∞

To show an example we take a multilayered medium characterized by permittivity contrasts only. The relative electric permittivity and layer thicknesses are given in Table 1. The first layer thickness indicates the height of the source and receivers in the upper half space above the upper most interface. The GPR data is modeled in 2D with TE-mode set up using a horizontal electric current line source and offsets between receivers and sources perpendicular to the source and receiver directions. From the electric and magnetic field receivers the upgoing wavefield is separated from the down going wavefield. The upgoing field is the electric field reflection response, $R(\mathbf{x}_r,\mathbf{x}'_r,t)$ and is shown in Figure 2(a). The direct transmission field field from receiver level to focus point $e_d^+(\mathbf{x}_r,\mathbf{x}_i,t)$ is directly computed from the model. These two fields are used in equations 27 and 28 to find the up- and downgoing parts of the focusing wavefield e_c^+, e^-. From these the up- and downgoing Green's functions are computed from equations 25 and 26. The focusing point is chosen in the middle of the fourth layer, half a meter below the thin layer at $\mathbf{x} = (0, 2.65)$ m. Three reflectors are above and below the focusing point. The retrieved response being the sum of $G^{\pm}(\mathbf{x}_i,\mathbf{x}_r,t)$ is shown in Figure 2(b) in red dashed lines overlaying the directly modeled response with a receiver at the focus point and the amplitudes are scaled by a factor t^2 to increase the coda visibility. From the figure it can be seen that both the primary reflections and the coda are very well retrieved with this scheme. This is achieved without having a receiver at that location, which makes our scheme stand out from existing Green's function retrieval schemes.

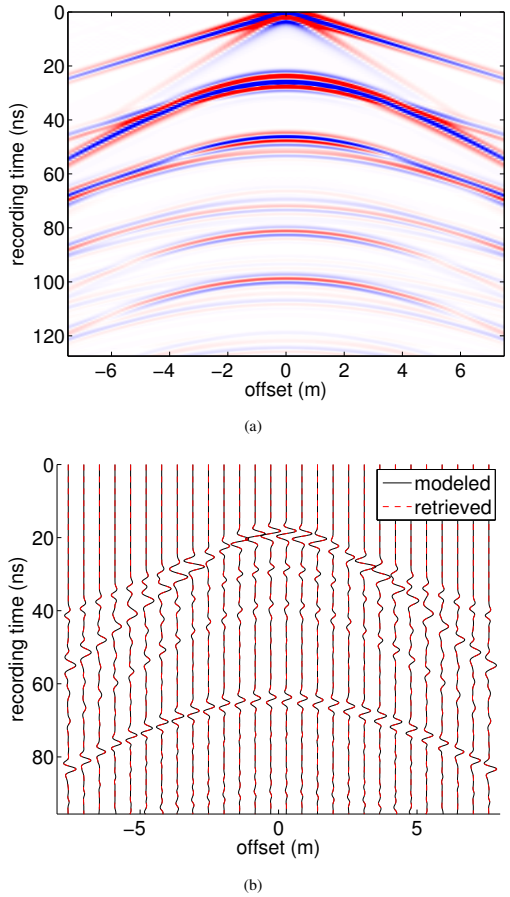

Figure 2: (a) Electric field normalized GPR reflection response $R(\mathbf{x}_r,\mathbf{x}'_r,t)$, (b) True (black solid lines) and retrieved (red dashed lines) electric field normalized GPR Green's function $G^+(\mathbf{x}_i,\mathbf{x}_r,t) + G^-(\mathbf{x}_i,\mathbf{x}_r,t)$.

WAVE FIELD IMAGING

For imaging the two Green's functions can be used, because they represent the wavefields that correspond to up- and downgoing waves at subsurface depth level z_i. The Green's functions are electric fields and therefore equation 12 holds. We can find the electric field reflection response as (Slob, 2009)

$$G^-(\mathbf{x}_i,\mathbf{x}_r,t) = \int_{\partial\mathbb{D}_i}\int_{t'=t_d(\mathbf{x}'_i,\mathbf{x}_r)}^{t} R(\mathbf{x}_i,\mathbf{x}'_i,t-t')G^+(\mathbf{x}_i,\mathbf{x}_r,t')\mathrm{d}t'\mathrm{d}\mathbf{x}'_T, \tag{30}$$

for $t \geq t_d(\mathbf{x}_i,\mathbf{x}_r)$. The reflection response to the layered medium that is the same as the actual medium below $\partial\mathbb{D}_i$ while it is homogeneous above $\partial\mathbb{D}_i$ is denoted $R(\mathbf{x}_i,\mathbf{x}'_i,t)$. The integration bounds are determined by causality of the reflection response and the Green's function. van der Neut *et al.* (2013) show that a more stable result can be obtained by changing equation 30 into a Fredholm integral equation of the second kind, by considering that the first arrival of $G^+(\mathbf{x}_i,\mathbf{x}_r,t)$ is the inverse of $e_d^+(\mathbf{x}_i,\mathbf{x}_r,t)$ which can be used when the downgoing Green's function is split in a direct arrival and a coda. Computing the reflection response for many points in the subsurface true amplitude images can be obtained by taking $R(x_i,x_i,t=0)$ for all desired image points $\mathbf{x}_i$, without ghost effects related to internal multiples in the data (Wapenaar *et al.* , 2012).

CONCLUSIONS

The recent extension of Marchenko equations to work in three-dimensional heterogeneous media has allowed us to derive two coupled Marchenko equations. The coupled equations make it possible to retrieve separately the upgoing and downgoing Green's functions corresponding to the electric wavefield generated by a source at or above the surface and recorded by a virtual receiver in the subsurface. For this we have derived an electric field formulation that restricts the lateral heterogeneities to be smooth. A numerical example shows that the scheme is capable to accurately retrieve the Green's functions including the scattering coda of the wavefield. We have shown how the separate retrieval of the directional Green's functions can be used in an imaging scheme that does not suffer from internal multiple scattering effects.

REFERENCES

Broggini, Filippo, Snieder, Roel, & Wapenaar, Kees. 2012. Focusing the wavefield inside an unknown 1D medium: Beyond seismic interferometry. *Geophysics*, **77**(5), A25–A28.

de Hoop, A. T. 1995. *Handbook of radiation and scattering of waves*. Amsterdam: Academic Press.

Kong, JA. 1972. Electromagnetic fields due to dipole antennas over stratified anisotropic media. *Geophysics*, **37**(6), 985–996.

Slob, E. 2009. Interferometry by deconvolution of multi-component multi-offset GPR data. *IEEE Transactions on Geoscience and Remote Sensing*, **47**(3), 828–838.

Slob, E.C., Draganov, D., & Wapenaar, K. 2007. Interferometric electromagnetic Green's functions representations using propagation invariants. *Geophysical Journal International*, **169**(1), 60–80.

Slob, Evert, Wapenaar, Kees, Broggini, Filippo, & Snieder, Roel. 2013. Seismic reflector imaging while eliminating internal multiples using Marchenko-type equations. *Geophysics*, **78** (Submitted), .

van der Neut, J., Slob, E., Wapenaar, K., Thorbecke, J., Snieder, R., Broggini, F., , Behura, J., & Singh, S. 2013. Interferometric redatuming of autofocused primaries and internal multiples. Presented at the 83rd Annual International meeting of the SEG.

Wapenaar, C. P. A., & Berkhout, A. J. 1989. *Elastic wave field extrapolation: Redatuming of single- and multi- component seismic data*. Advances in Exploration Geophysics. Elsevier Science Publishers.

Wapenaar, K. 2004. Retrieving the elastodynamic Green's function of an arbitrary inhomogeneous medium by cross correlation. *Physical Review Letters*, **93**(25), 254301.

Wapenaar, K., Thorbecke, J., van der Neut, J., Slob, E., Broggini, F., & Snieder, R. 2012. Integrated migration and internal multiple elimination. *SPMUL1.5 of: SEG Technical Program Expanded Abstracts*.

Wapenaar, K., Slob, E., Broggini, F., Snieder, R., Thorbecke, J., & van der Neut, J. 2013. Data-driven Green's function retrieval from reflection data: theory and example. Presented at the 83rd Annual International meeting of the EAGE.

Wapenaar, K., Slob, E., van der Neut, J., Thorbecke, J., Broggini, F., & Snieder, R. 2013a. Three-dimensional Marchenko equation for Green's function retrieval "beyond seismic interferometry". Presented at the 83rd Annual International meeting of the SEG.

Wapenaar, Kees, Broggini, Filippo, Slob, Evert, & Snieder, Roel. 2013b. Three-Dimensional Single-Sided Marchenko Inverse Scattering, Data-Driven Focusing, Green's Function Retrieval, and their Mutual Relations. *Physical Review Letters*, **110**(Feb), 084301.

Weaver, R. L., & Lobkis, O. I. 2001. Ultrasonics without a source: Thermal fluctuation correlations at MHz frequencies. *Physical Review Letters*, **87**(13), 134301.